Monte Carlo Study of Symmetric Diblock Copolymers in Nonselective Solvents

Luis A. Molina, Antonio López Rodríguez, and Juan J. Freire*

Departamento de Química Física, Facultad de Ciencias Químicas, Universidad Complutense, 28040 Madrid, Spain

Received August 2, 1993; Revised Manuscript Received November 29, 1993®

ABSTRACT: Monte Carlo simulations have been performed with a lattice model that represents systems of symmetric diblock copolymer chains immersed in a nonselective solvent of varying thermodynamic quality. Different values for the polymer concentration and the energy parameter that gauges solvent quality have been set. This way, the chain dimensions and the solvent segregation and microphase separation transitions have been numerically characterized for two different chain lengths. The results are discussed and compared with existing theoretical predictions (mean-field and self-consistent-field treatments for Gaussian chains).

Introduction

Block copolymer systems (solutions and melts) are of special interest, since they exhibit peculiar properties concerning ordering and phase separation.[1] The mean-field[2] and self-consistent-field[3] theories for symmetric diblock (A–B) copolymers in nonselective solvents predict ordered lamellar structures, which are reached from disordered states by means of microphase separation transitions (MSTs). These theories are based in the weak segregation limit regime, valid for both the disordered phase and the ordered phase, in conditions near the MST, where the boundaries between microdomains are not sharply defined and the individual copolymer chains are only slightly perturbed from their ideal (Gaussian) behavior. On the other hand, strong segregation limit theories[4,5] have been proposed to deal with well-developed ordered structures with sharp interfaces and individual chain stretching, characteristic of concentrated solutions or melts of long polymers at low temperatures, far away from the MST, which have also been investigated in recent experimental work.[6]

Very recently, regular diblock copolymer systems have been the aim of an extensive Monte Carlo simulation by Binder et al.[7,8] This numerical work seems to confirm the main features of the MST, though a noticeable stretching is also observed for the chain dimensions. The numerical algorithms employed in the simulation studies contemplate a certain proportion of vacancies in the lattice, which allow for the appropriate chain motions. However, in these simulations, the fraction of vacancies, ϕ_v, was kept small in order to prevent polymer–solvent unmixing (the most detailed calculations[8] were, in fact, performed without any consideration of attractive interactions between polymer units of the same type, A–A or B–B, which is equivalent to assume a good, nonsegregating solvent). Notwithstanding, if the fraction of vacancies is increased, one can describe copolymer solutions where the polymer volume fraction ϕ, i.e., $1 - \phi_v$, and the balance between different interactions A–A, B–B, and A–B determine the occurrence of solvent segregation and (or) MST.

In the present paper, we have undertook the Monte Carlo simulation of these complicated types of systems. Thus, we consider symmetric diblock copolymers of two different lengths, or total number of units, N, immersed in a nonselective solvent. These systems are investigated as the first step in the general study of copolymers in different types of selective solvents. We obtain properties (such as the chain mean dimensions and magnitudes related to the collective scattering factor, $S_{col}(\mathbf{q})$, depending on the scattering vector $\mathbf{q}$) for varying concentrations and solvent conditions. This way, we can sketch phase transition diagrams and establish correlations between conformational properties of individual chains and the system macroscopic state. As in the simulations previously mentioned,[7,8] the MST is characterized by studying the functions $S_{copo}(\mathbf{q})$ obtained with two opposite contrast factors for scattering centers A and B.[9] In order to investigate the solvent segregation, we have performed an analysis of the results for a collective scattering function, $S_{pol}(\mathbf{q})$, which has been obtained assuming the same contrast factors for A and B units (and an adequate opposite factor for the solvent). These results for the "optical homopolymer" system are then analyzed according to the scheme which we followed in a previous work[10] concerning the numerical prediction of phase separation curves for homopolymer solutions. The practical differences between the definitions of $S_{copo}(\mathbf{q})$ and $S_{pol}(\mathbf{q})$ will be detailed in paragraphs b1 and b2 of the Methods section.

Methods

The chain model employed through this work was detailed in a previous paper devoted to homopolymer chains.[11] We place n self-avoiding, monodisperse chains of N units (the present results correspond to N = 36 and 60) in a simple cubic lattice. Solvent units are assumed to occupy the remaining lattice sites (vacancies). Two blocks of $N/2$ units, one with units of type A and the other containing B units, are distinguished in each chain. We consider attractive interactions gauged by the parameter $\epsilon/(k_BT)$ for every pair of nonbonded units of the same type (A–A or B–B) which are at adjacent lattice sites in a given configuration. This way, we mimic the attractive interactions between chain monomers of the same type. A–B or polymer–solvent attractive interactions are not included in the model so that $\epsilon/(k_BT)$ can describe simultaneously the solvent quality and also the effective repulsion between units A and B (which tend to segregate, given their different compositions). Thus, at high temperature, solvent and A–B segregation effects are suppressed. At lower temperatures, both effects compete as phase transitions occur. Periodic boundary conditions are introduced in the customary way. The number of chains in the system and the polymer volume fraction are directly related, since $\Phi = nN/n_s$, where n_s is the total number of lattice sites, $n_s = L^3$ (L is the box size or cube length). Then, an adequate election of the box size[12] determines the minimum number of chains necessary to give a reasonably accurate description of the system.

We have made use of a Monte Carlo algorithm also previously detailed.[11] The conformations are generated by means of reptations or, alternatively, local motions or kink jumps (i.e.,

® Abstract published in *Advance ACS Abstracts*, February 1, 1994.

0024-9297/94/2227-1160$04.50/0

bends, crankshafts, or end motions, depending on the selected unit) applied to a chain, which is randomly chosen at every Monte Carlo cycle. The proportion between reptations and kink jumps is conveniently optimized. A previous thermal equilibration of the system is performed. The Metropolis criterion is used to decide the acceptance or rejection on new configurations (for which the single occupation rule has been previously enforced). Properties are finally calculated as arithmetic means over a selected sample constituted by the configurations obtained every certain number of steps (10^4 or 2×10^4), within runs extended over several tens of thousands of Monte Carlo cycles. (A Monte Carlo cycle is defined as the averaged number of steps for which all the polymer units have changed their positions, and therefore, it is set here to be a number of configurations equal to the number of polymer sites in the system.)

We evaluate the following properties.

(a) Mean Quadratic Radius of Gyration. We characterized the individual chain dimensions by means of this average, $\langle R_g^2 \rangle$, calculated from the quadratic radius of gyration, obtained for every one of the chains constituting the system, in the different configurations within the sample, according to the definition

$$R_g^2 = (1/N^2)\sum_{i}^{N}\sum_{j}^{N}(\mathbf{R}_i - \mathbf{R}_j)^2 \tag{1}$$

where $\mathbf{R}_i$ is the position vector of unit i in a given chain.

(b) Collective Scattering Functions. These functions are obtained (in reduced form) from the general expression

$$S^*_{col}(\mathbf{q}) = L^{-3}\langle [\sum_{i}^{n_s} f^*_i \cos(\mathbf{q}\cdot\mathbf{R}_i)]^2 + [\sum_{i}^{n_s} f^*_i \sin(\mathbf{q}\cdot\mathbf{R}_i)]^2 \rangle \tag{2}$$

f^*_i represent a contrast factor proportional to the difference between the local refractive index in site i and the solution refractive index.[9,10] The values of the components of $\mathbf{q}$ for which the evaluation of S^*_{col} is feasible are limited by the box size so that the condition

$$q_j = (2\pi/L)k_j \qquad k_j = 0, 1, 2, \ldots \tag{3}$$

is imposed on every one of the three components ($j = x, y, z$) of the scattering vector, $\mathbf{q}$.

Assuming a linear variation of the refractive index with Φ, we can use convenient expressions for $f^*_i(\Phi)$ in two interesting different cases.

(1) Optical Homopolymer. We assign identical refractive indices to units A and B, different from the solvent refractive index. Then, as stated in the case of a homopolymer chain[10]

$$f^*_i = -\Phi \tag{4a}$$

if site i is occupied by solvent (i.e., it is a void or vacancy), and

$$f^*_i = 1 - \Phi \tag{4b}$$

if site i is occupied by a polymer unit (A or B). This way, we obtain the corresponding functions, denoted as $S_{pol}(\mathbf{q})$.

(2) Optical Copolymer. In this case, we assign refractive indices to A and B so that the differences with respect to the solvent refractive index are the same but of opposite signs. Consequently, $f^*_i = 1, 0, -1$ for sites respectively occupied by A, solvent (voids), and B units. This is the situation considered in previous simulations for copolymer systems.[7,8] The functions obtained with these prescriptions are denoted as $S_{copo}(\mathbf{q})$.

From the functions $S_{copo}(\mathbf{q})$, we also obtained some other magnitudes useful to characterize the system anisotropy and, therefore, to give an indication of the occurrence of ordering. These magnitudes have been described in previous simulation work for copolymers.[8] Following this description, $S_{copo}(\mathbf{q})$ corresponds to a fictitious mass distribution in the q space, from which one can obtain its moment-of-inertia tensor in a given configuration. Explicitly, the elements of this 3×3 tensor are calculated as

$$T_{ii}^{conf} = \sum^{k_m} S_{copo}^{conf}(\mathbf{q})q_j^2 \tag{5a}$$

$$T_{ij}^{conf} = -\sum^{k_m} S_{copo}^{conf}(\mathbf{q})q_i q_j \qquad i \neq j \tag{5b}$$

$$i, j = x, y, \text{or } z$$

where the sums $\sum^{k_m}$ extend over the values of k_j or k_i (from 1 to the maximum value included in the calculations, k_m) for which the different components of $\mathbf{q}$ (q_x, q_y, and q_z) are set, according to eq 3. The eigenvalues and eigenvectors of tensor $\mathbf{T}^{conf}$ are then computed. The normalized principal direction (i.e., the eigenvector corresponding to the smallest eigenvalue), T_1^{conf}, for the given configuration is then stored. Once all the configurations have been generated, we compute the correlation function

$$C_q(\tau) = \langle |T_1^{conf}(t)\cdot T_1^{conf}(t+\tau)| \rangle_t - 1/2 \tag{6}$$

where t denotes the Monte Carlo cycle which corresponds to a given configuration within the sample and the term $-1/2$ is included so that the function vanishes for high values of τ. Variable t can be assumed to be proportional to time if our sample represents a "dynamic" Monte Carlo trajectory. (Unit time is defined in terms of a Monte Carlo cycle.) Then, assuming a single relaxation process, we can estimate a normalized relaxation time, as the value τ_q, for which $C_q(\tau_q)$ decreases from its initial value, 1/2, to $1/2e = 0.188$. A value of τ_q significantly higher than those obtained for homogeneous systems (i.e., for small values of ϵ or ϕ) indicates that the configurational anisotropy persists along with time. Therefore, $\tau_q \gg 0$ is associated to equilibrium ordered structures.

Results and Discussion

(a) Dimensions. The results for $\langle R_g^2 \rangle$ obtained with copolymer chains of 36 and 60 units are contained in Tables 1 and 2. The lowest values of Φ correspond to a single chain in the system. In this case, we observe a transition from the excluded volume regime, $\epsilon/(k_B T) \simeq 0$ or good solvent conditions, where the chains behave as expanded coils, to a more compact (collapsed) structure at lower temperatures. However, this collapse is more gradual than in the case of homopolymer chains with the same number of units,[11] as it is in part prevented by the segregation between the A and B blocks. In the good solvent conditions, an increase of the chain concentration tends to compensate the intramolecular interactions (i.e., the excluded volume effects). Therefore, $\langle R_g^2 \rangle$ decreases for higher values of Φ as the chains try to mimic their unperturbed of quasi-ideal dimensions. According to our previous work with the same model,[11] a single homopolymer chain reaches its unperturbed state at $\epsilon/(k_B T) = 0.275$ (Θ temperature). However, comparing the present results in Tables 1 and 2 with those in Table II of ref 11, it can be noticed that the copolymer values of $\langle R_g^2 \rangle$ at this temperature are increased with respect to the homopolymer unperturbed dimensions by a factor of $\gamma \simeq 1.10$–1.15. Recent renormalization group treatments[13,14] predict $\gamma \simeq 1.19$ for very long chains. We have performed a more detailed numerical study of this point, using Monte Carlo algorithms and models which are specifically efficient for isolated chains.[15] These more refined calculations yield results for γ which converge to a constant value, close the theoretical one, as N increases, when the interactions between units belonging to the same block are ignored (as in the theoretical models). However, the copolymer chains show a slight excluded volume effect at the homopolymer Θ temperature, when we introduce A–A and B–B interaction effects (as in the model used in this work). The present data for nondilute systems also show an interesting feature at the homopolymer Θ temperature; there is little

Table 1. Results for $\langle R_g^2 \rangle$ Obtained with $N = 36$

	ϕ						
$\epsilon/(k_BT)$	0[a]	0.036	0.11	0.22	0.38	0.52	0.75
0.1	12.0	11.8	11.5	10.9	10.4	10.1	9.6
0.2	11.5	11.5	11.2	10.5	10.2	9.9	9.7[c]
0.275	10.6	10.5	10.4	10.4	10.3[c]	10.4[c]	10.4[c]
0.3	10.4	10.4	10.5	10.3	10.5[c]	10.6[c]	10.5[c]
0.4	9.9	9.9	10.1	10.3[c]	10.7[c]	11.1[c]	10.7[c]
0.5	9.1	9.3	9.8	10.6[b]	11.3[b]	11.1[b]	10.9[c]
0.6	8.6	8.9	10.2[b]	11.4[b]	11.5[b]	11.6[b]	11.2[c]
0.8	7.3	8.9	10.5[b]	11.2[b]	11.6[b]	11.2[b]	10.3[c]

[a] Single chain. [b] Phase separation (solvent segregation). [c] Microphase separation.

Table 2. Results for $\langle R_g^2 \rangle$ Obtained with $N = 60$

	ϕ						
$\epsilon/(k_BT)$	0[a]	0.038	0.15	0.22	0.39	0.50	0.76
0.1	21.3	20.7	19.5	19.1	18.3	17.8	16.7
0.2	19.8	19.2	19.0	18.6	18.0	18.6[c]	17.6[c]
0.275	18.5	18.2	18.2	18.5	18.6[c]	19.1[c]	18.0[c]
0.3	18.2	18.1	17.8	18.2	19.5[c]	18.5[c]	17.3[c]
0.4	16.4	16.8	17.4	18.7[c]	19.2[c]	19.3[c]	17.5[c]
0.5	14.6	15.3	17.9[b]	18.9[b]	17.9[b]	18.3[b]	17.2[c]
0.6	12.9	14.0[b]	17.1[b]	17.6[b]	17.8[b]	17.0[b]	17.0[c]

[a] Single chain. [b] Phase separation (solvent segregation). [c] Microphase separation.

variation of the copolymer dimensions with Φ, at low or moderate concentrations, in contrast with the sharper changes found at higher or lower values of $\epsilon/(k_BT)$.

Away from the dilute or good solvent limits, the results in Tables 1 and 2 reveal an increase in dimensions as ϵ/k_BT) and Φ increase. This increase can be associated with the chain stretching in ordered structures close to (or beyond) the MST transition.[7,8] At the highest concentrations, we observe that this stretching effect is smaller and the dimensions decrease again. For these concentrated systems, every block approaches the ideal dimensions since it is surrounded by many other units of the same type, belonging to neighboring chains, and this mean-field effect is in competition with the chain stretching.

Moreover, it should be considered that some of the results in Tables 1 and 2 (especially the results obtained with the highest values of $\epsilon/(k_BT)$ correspond to systems for which solvent segregation occurs (as will be shown below). For these cases, the reported dimensions should be interpreted as averages over the values corresponding to the dilute phase (a few chains in the collapsed state) and those associated to the chains in a more concentrated homogeneous solution. This explains the decrease of stretching effects observed for some of the systems as temperature decreases, in the low-temperature range.

(b) Macroscopic Phase Separation (Solvent Segregation). The results obtained with our copolymer systems for $S_{pol}(\mathbf{q})$ (i.e., corresponding to the optical homopolymer scattering function) have been analyzed in order to characterize solvent segregation. This analysis has been performed according to a method detailed in previous work for homopolymer systems (an abundant graphical illustration of this method can be found in ref 10). The main steps of the procedure are as follows: We consider systems with chains of a given length, N, and different temperatures and concentrations. For every one of these systems, we plot $S_{pol}^{-1}(q)$ vs q^2. From these plots, we perform extrapolation to $q = 0$. This way, we estimate the magnitude $S_{pol}(q=0)$, which should diverge for systems meeting the spinodal curve conditions. Therefore, negative values of $S_{pol}^{-1}(q=0)$ are indicative of phase separation. Then, we can select the temperatures for which there is

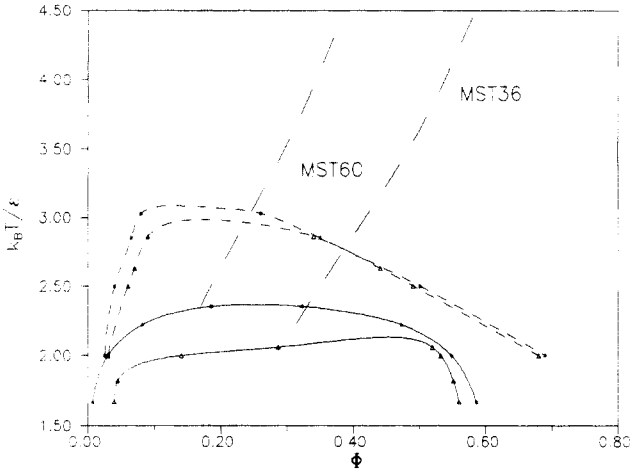

Figure 1. Solvent segregation curves for the $N = 36$ (△) and $N = 60$ (*) copolymer chain systems (solid curves), compared with similar curves obtained previously for homopolymer chains[10] (short-dash curves). The regions beyond the MST for the $N = 36$ and $N = 60$ chains are also delimited (long-dash curves).

a range of intermediate concentrations where solvent segregation is manifested. A plot of $S_{pol}^{-1}(q=0)$ vs Φ for every one of these temperatures provides a pair of numerically interpolated values of the concentration which meets the spinodal curve conditions, $S_{pol}^{-1}(q=0) = 0$.

We show in Figure 1 the spinodal curves corresponding to the $N = 36$ and 60 systems. These curves were drawn according to standard spline interpolation techniques. They can only be considered as semiquantitative estimations, given the uncertainties associated with the different extrapolations and interpolations employed to characterize the spinodal points. However, they are able to provide a good description of the most relevant effects concerning polymer composition or chain length dependence. Similar curves obtained previously for the homopolymer[10] are also included for comparison. A remarkable decrease of the critical temperature (i.e., maximum in the spinodal curve, above which there is no phase separation at any concentration) can be observed for the copolymer systems. This decrease can be explained by the competition between repulsive polymer–solvent and A–B interactions. Macroscopic phase separation decreases the former interactions but causes a more dense packing of copolymer chains, which increases the nonfavorable A–B contacts. Then, solvent segregation loses its efficiency to lower the free energy with respect to the case of homopolymer systems. Of course, the critical temperature increases for the longest chain. However, the difference between the homopolymer and copolymer critical temperatures is smaller for this chain. It is not clear at present whether the homopolymer and copolymer critical temperatures should converge for infinitely long chains, given a common Θ temperature. (This limit, on the other hand, corresponds to the maximum differentiation between the homopolymer and copolymer systems.) Alternative definitions of the Θ temperature do not clarify this point. Thus, as explained in the discussion for dimensions, a proportionality between $\langle R_g^2 \rangle$ and N is still expected for isolated copolymer chains constituted by two unperturbed blocks with repulsive interactions between them,[13-15] though slight excluded volume effects are observed[15] at the homopolymer Θ temperature for models of isolated copolymer chains in which A–A and B–B interactions have been explicitly introduced. In any case, the present phase separation data indicate that the depression in the copolymer critical temperature can be important for moderately long chains.

The critical volume fraction is smaller for the longest chain ($N = 60$). This effect is common for homopolymer and copolymer systems.[10] However, the copolymer systems (especially for $N = 36$) exhibit flatter curves, and therefore, this critical concentration cannot be precisely determined.

(c) Microphase Ordering. Our study of the microphase ordering is mainly based on the results obtained for $S_{copo}(\mathbf{q})$ (i.e., the scattering functions for optical copolymers). This function is zero for $q = 0$ and, therefore, exhibits a maximum[9] for an intermediate value of q, q^*. Ordered structures are characterized by the divergence of this peak.[2]

Following the methods prescribed in the analysis of previous simulations[8] by Binder et al., we have performed least-squares fits of our numerical data to the nonlinear function

$$S_{copo}^{-1}(\mathbf{q}) = (1/N\alpha)[F(q\tilde{R}_g) - \delta] \quad (7)$$

where α, δ, and $\tilde{R}_g$ are the fitting parameters. These fits, not shown explicitly here, were performed according to standard numerical techniques.[16] $F(x)$ is defined as[2,8]

$$F(x) = (x^4/2)[(x^2/4) + e^{-x^2/2} - (1/4)e^{-x^2} - (3/4)]^{-1} \quad (8)$$

which has a maximum at $x^* = 1.95$, i.e., $q^* = 1.95/\tilde{R}_g$.

Equation 7 is justified from the mean-field prediction for the structure factor, valid for a system with randomly distributed vacancies, in the weak segregation limit. According to it, the theoretical values for these parameters are[8]

$$\alpha = 4\phi \quad (9)$$

$$\delta = 2\phi\chi N \quad (10)$$

and

$$\tilde{R}_g = \langle R_g^2 \rangle^{1/2} \quad (11)$$

or

$$q^* = 1.95/\langle R_g^2 \rangle^{1/2} \quad (12)$$

χ is the Flory interaction parameter, which describes the system mean interaction between A and B groups. For our model, neglecting end chain effects and accounting properly for the total number of A–B (or B–A) contacts,

$$\chi = (z - 2)\epsilon/(k_B T) \quad (13)$$

where z is the lattice coordination number ($z = 6$ for the simple cubic lattice). (In ref 10, we defined χ as the parameter for polymer–solvent interactions in homopolymer systems. The relaxation between χ and ϵ for this alternative definition differs in an extra 1/2 factor from eq 13.)

Negative values for $S_{copo}^{-1}(q^*)$ are sometimes obtained from the fitting results, and these values are immediately associated with clearly divergent peaks. In Tables 3 and 4, we present a summary of the fitting results for the systems with chain lengths $N = 36$ and 60, together with the scattering function at the peak, $S_{copo}(q^*)$.

According to the mean-field theory,[2] the symmetric diblock copolymers should have a MST transition to ordered lamellar structures at the value of the Flory parameter, χ_t, corresponding to $\chi_t N\phi_t \simeq 10.5$. The Hartree corrections[3] to this theory yield

Table 3. Results from the Scattering Function for Optical Copolymers of 36 Units

$\epsilon/(k_BT)$	ϕ	$N\chi\phi$	α/ϕ	$\delta/(N\chi\phi)$	$q^*\langle R_g^2\rangle^{1/2}$	$S_{copo}(q^*)/\phi$	τ_q
0.1	0.036	0.52	5.2	−1.5	1.93	8.6	<10
	0.11	1.58	4.3	2.5	2.01	9.0	7
	0.22	3.16	4.0	3.1	1.87	12.8	7
	0.38	5.48	3.5	1.6	1.95	10.4	11
	0.52	7.38	4.7	1.0	1.79	12.5	17
	0.75	10.8	5.3	0.7	1.66	14.1	84
0.2	0.036	1.06	4.6	2.4	1.94	8.9	<10
	0.11	3.16	4.4	1.6	1.89	9.8	7
	0.22	6.32	4.0	1.5	1.83	12.8	9
	0.38	11.0	3.5	1.3	1.71	18.0	17
	0.51	14.8	3.4	1.1	1.72	23.5	36
	0.75	21.5	2.56	0.9	1.76	70	370
0.275	0.036	1.44	4.4	2.3	1.93	9.2	<10
	0.11	4.34	4.7	1.0	1.87	10.2	7
	0.22	8.70	4.7	1.0	1.71	13.8	13
	0.38	15.1	4.0	0.9	1.67	20.8	30
	0.51	20.3	4.7	0.7	1.76	40.8	113
	0.75	29.6	3.4	0.5	1.59	25	1000
0.4	0.036	2.24	4.2	2.5	1.94	9.8	<10
	0.11	6.32	3.8	1.8	1.89	14.4	15
	0.21	12.6	3.7	1.7	1.81	21.4	31
	0.38	21.9	3.8	0.8	1.68	42	114
	0.51	29.5	3.0	0.7	1.68	98.1	1000
	0.75	43.0	2.8	0.5	1.54	253	>2000
0.5	0.036	2.64	4.0	2.9	1.90	10.9	22
	0.11	7.92	3.8	1.9	1.78	22.1	41
	0.22	15.8	3.1	1.2	1.81	33.7	161
	0.38	26.6	2.6	0.8	1.67	315	>1000
	0.52	37.1	3.0	0.5	1.57	40	>3000
	0.75	53.8	1.4	0.4	1.77	D[a]	>3000
0.6	0.036	3.16	4.7	2.8	1.85	14.2	44
	0.11	9.5	4.4	1.6	1.60	47	1000
	0.22	19.0	3.9	1.0	1.70	159	>3000
	0.38	32.9	2.1	0.7	1.81	D[a]	>3000
	0.52	44.3	1.0	0.4	1.95	D[a]	>3000
	0.75	64.8	1.0	0.4	1.98	D[a]	>3000
0.8	0.038	4.22	7.6	2.5	1.74	27	>1000
	0.11	12.7	6.0	1.4	1.67	88	>3000
	0.22	25.4	2.0	0.8	1.94	163	>3000
	0.38	44	4.1	0.5	1.75	142	>3000
	0.52	59	2.2	0.3	1.76	92	>3000
	0.74	86	1.2	0.2	1.93	D[a]	>3000

[a] Negative result indicating divergence of the scattering function.

$$\chi_t N\phi_t = 10.5 + 41\tilde{N}^{-1/3} \quad (14)$$

where $\tilde{N} = N(6\langle R_g^2\rangle/N)^3\Phi_t^2$.

The values of the fitting parameter α in Tables 3 and 4 are in general in good agreement with eq 9, in the case of systems for which solvent segregation or strong segregation has not taken place. The values of δ are systematically smaller than the mean-field theory result (eq 10). The Hartree theory for finite chains predicts[3,8] high corrections to the mean-field value. These corrections should be negative and proportional to $\tilde{N}$, which is roughly confirmed by our results, though a quantitative verification of this improved theory cannot be accurately established with the present fitting values. Moreover, we find that some dilute systems show results for δ very different from those obtained for moderate or high values of ϕ. However, since the right side in eq 10 is small for these systems and the uncertainties in δ are estimated to be at least ±2 (according to the previous estimations for good solvent systems[8]), these deviations can be a consequence of numerical error.

We observe a significant variation of the values obtained for $q^*\langle R_g^2\rangle^{1/2}$ with respect to the mean-field result, 1.95. The values become considerably smaller for systems close to the MST or for systems with ordered structures. In spite of the high uncertainties of these values, they seem

Table 4. Results from the Scattering Function for Optical Copolymers of 60 Units

$\epsilon/(k_BT)$	ϕ	$N\chi\phi$	α/ϕ	$\delta/(N\chi\phi)$	$q^*\langle R_g^2\rangle^{1/2}$	$S_{copo}(q^*)/\phi$	τ_q
0.1	0.038	0.88	4.8	0.7	1.93	14.2	7
	0.15	3.60	4.3	0.9	1.93	14.7	8
	0.22	5.40	4.3	1.1	1.88	17.3	11
	0.39	9.4	4.0	1.0	1.88	20.1	14
	0.50	11.9	4.5	0.9	1.72	26.8	43
	0.76	18.4	3.02	1.1	1.72	288	32
0.2	0.038	1.78	5.2	0.	1.84	14.7	13
	0.15	7.20	4.6	0.9	1.79	21	13
	0.22	10.8	4.1	0.9	1.86	22	13
	0.39	18.7	4.4	0.8	1.65	42	53
	0.50	23.8	3.1	1.0	1.74	84	182
	0.76	36.7	3.1	0.5	1.76	140	>1000
0.275	0.038	2.44	3.8	3.1	2.00	16.6	13
	0.15	9.9	3.1	1.3	1.99	23.3	18
	0.22	14.9	4.4	0.8	1.74	28	26
	0.39	25.8	3.1	0.7	1.73	86	260
	0.50	32.7	3.4	1.1	1.57	D[a]	535
	0.76	50.5	2.4	0.5	1.60	1000	>3000
0.4	0.038	3.56	3.8	2.2	1.94	18	20
	0.15	14.4	4.2	0.9	1.89	31	55
	0.22	21.6	4.0	0.8	1.71	160	250
	0.39	37.4	3.1	0.5	1.68	141	>3000
	0.50	47.6	2.8	0.9	1.67	D[a]	>3000
	0.76	73.4	1.0	0.6	1.94	D[a]	>3000
0.5	0.038	4.44	4.0	2.4	1.85	23.4	80
	0.15	18.0	5.0	0.9	1.77	80	422
	0.22	27.0	2.6	1.6	1.9	D[a]	>3000
	0.39	46.8	2.6	0.5	1.8	D[a]	>3000
	0.50	59.4	2.0	0.4	1.8	D[a]	>3000
	0.76	91.8	1.5	0.2	2.2	D[a]	>3000
0.6	0.038	5.32	4.0	3.2	1.83	54	1540
	0.15	21.6	6.4	1.4	1.71	56	1000
	0.22	32.4	2.6	1.1	1.47	89	>3000
	0.39	56.2	2.0	0.4	1.77	D[a]	>3000
	0.50	97	3.3	0.0	1.35	D[a]	>3000
	0.76	110	2.3	0.2	1.89	D[a]	>3000

[a] Negative result indicating divergence of the scattering function.

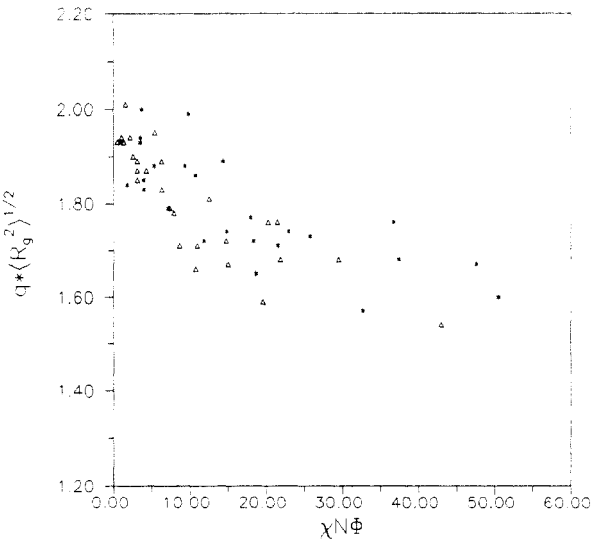

Figure 2. Scaled peak positions, q^*, for the function $S_{copo}(q)$ vs the scaling variable $\chi N\phi$. (Δ) $N = 36$, (*) $N = 60$. (Systems with strong solvent segregation are excluded.)

to vary as a universal function of $\chi N\phi$ (see Figure 2). This trend was also observed for copolymers in good solvents at a single, high concentration[8] and represents a discrepancy with respect to the weak segregation theories. As can be expected, the results deviate from the universal behavior for very concentrated systems or for the systems exhibiting solvent segregation. (The other fitting parameters also show more irregular patterns in these cases.)

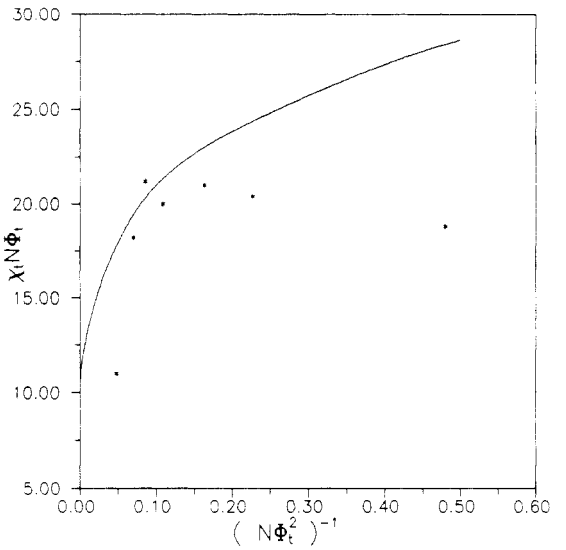

Figure 3. Results obtained for χ_t and Φ_t from our characterization of the MST (*), plotted for quantitative comparison with the self-consistent-field theory prediction, eq 14 (solid curve).

The results for $S_{copo}(q^*)/\Phi$ can also be compared with the results for τ_q, contained in the last columns of Tables 3 and 4. High values of these magnitudes (or a divergence for the scattering function) are characteristic of ordered structures. We observe that the variations of the two sets of results with the system parameters follow similar tendencies, which allow us to tentatively characterize the MST to an anisotropic (lamellar) structure. Since the values of τ_q exhibit a regular variation with ϕ and N, we have adopted this magnitude to gauge the system ordering. This way, we postulate that the system is clearly ordered (close or beyond the MST) when $\tau_q > 100$ time units, which, in the systems without solvent segregation, is equivalent to an increase of $S_{copo}(q^*)/\Phi$ by about 3 times its value for dilute and totally disordered systems. (This value is, as expected, approximately proportional to N.) Then, we have plotted τ_q vs ϕ for the systems corresponding to different values of N and $\epsilon/(k_BT)$ and have interpolated the volume fraction, ϕ_t, for which $\tau_q = 100$. From eq 13, we then determine $\chi_t N\phi_t$.

In Figure 1, we include curves that we estimate can delimit the MST, according to the $\tau_q = 100$ criterion. These curves always satisfy the $\chi_t N\phi_t > 10.5$ condition. In Figure 3, we present a plot in which our estimations for the MST are compared with the Hartree theoretical prediction, eq 14. Our results agree with the theory at the intermediate range of values of $\chi_t N\phi_t$, but strong deviations are observed for the low and high $\chi_t N\phi_t$ limits. Of course, this comparison should be considered with some caution, given the high uncertainties associated with our numerical determination of the MST conditions.

Nevertheless, some general features can be safely discussed from the transition curves sketched in Figure 1. It can be observed that the ordered structures can be obtained even for values of k_BT/ϵ above the homopolymer Θ temperature, for moderately concentrated systems. The critical concentration is displaced beyond the MST transition both for the $N = 36$ and the $N = 60$ copolymer chains.

Acknowledgment. We are grateful to C. Vlahos and A. Horta (UNED) for helpful discussions and comments. This research was supported by Grant PB92-0227 of the DGICYT (Spain).

References and Notes

(1) Bates, F. S. *Science* **1991**, *251*, 898.
(2) Leibler, L. *Macromolecules* **1980**, *13*, 1602.
(3) Fredickson, G. H.; Leibler, L. *Macromolecules* **1989**, *22*, 1238.
(4) Helfand, E.; Wasserman, Z. R. In *Developments in Block and Graft Copolymers-1*; Goodman, I., Ed.; Applied Science: New York, 1982.
(5) Semenov, A. N. *Sov. Phys. JETP* **1985**, *61*, 733.
(6) Matsushita, Y.; Mori, K.; Saguchi, R.; Noda, I.; Nagasawa, M.; Chang, T.; Glinka, J.; Han, C. C. *Macromolecules* **1990**, *23*, 4387.
(7) Minchau, B.; Dünweg, B.; Binder, K. *Polym. Commun.* **1990**, *31*, 348.
(8) Fried, H.; Binder, K. *J. Chem. Phys.* **1991**, *94*, 8349.
(9) Burchard, W.; Kajiwara, K.; Nerger, D.; Stockmayer, W. H. *Macromolecules* **1984**, *17*, 222.
(10) López Rodríguez, A.; Freire, J. J.; Horta, A. *J. Phys. Chem.* **1992**, *96*, 3954.
(11) López Rodríguez, A.; Freire, J. J. *Macromolecules* **1991**, *24*, 3578.
(12) Kremer, K. *Macromolecules* **1983**, *16*, 1632.
(13) McMullen, W.; Freed, K.; Cherayil, B. *J. Chem. Phys.* **1987**, *86*, 4280.
(14) Sdranis, Y.; Kosmas, M. K. *Macromolecules* **1991**, *24*, 1341.
(15) Vlahos, C.; Horta, A.; Molina, L. A.; Freire, J. J. Manuscript in preparation.
(16) Press, W. H.; Flannery, B. P.; Tenkolsky, S. A.; Vetterling, W. T. *Numerical Recipes*; Cambridge University Press: Cambridge, U.K., 1986.